Research Project Report

Investigation of a Solid Fuel Ramjet Projectile

Itamar Levitan

Advisor: Prof. Alon Gany

Faculty of Aerospace Engineering, Technion- Israel Institute of Technology

April 2024

Abstract

This research will revolve around the topic of Solid Fuel Ramjets (or SFRJ for short). The ramjet is a type of an airbreathing engine for high supersonic velocities (M>2.5) utilizing aerodynamic compression in the form of shockwaves, and introducing high energetic characteristics (Specific Impulse or I_{sp} in short) compared to other types of engines in supersonic Mach numbers. It has been found in previous studies that the SFRJ can be integrated onto different gun-launched projectiles as a form of self-propulsion, due to a simple design and operational characteristics fit for a gun-launched trajectory. Different theoretical, and experimental investigations have shown the feasibility of such propulsion systems to be integrated onto gun-launched projectiles, and dramatically increase the ballistic properties (range, impact velocity, and trajectory) of the projectile. This part of the research is only the theoretical, and logistical groundwork, needed in order to perform the series of experiments, necessary to analyze the characteristics of such propulsion systems, examining the internal ballistics and flameholding characteristics of the engine.

1. Introduction and Literature review

The concept of airbreathing propulsion systems has revolutionized the propulsion industry, in both fields of transportation and weaponry. Among the airbreathing propulsion systems, the solid fuel ramjet (SFRJ) is the simplest propulsion system there is, the air compresses itself and there isn't any fuel control. The SFRJ was found to be naturally tailored into missions of high-caliber gun-launched projectiles. In this work we will conduct a theoretical and experimental investigation of a gun launched SFRJ round and analyze its performance and characteristics.

1.1. Fundamentals of a propulsion system

In this section I will introduce some of the most basic characteristics of a propulsion system. These are the characteristics which dictate the performance of the engine, mostly range and velocity. We can describe them using Specific Impulse (Isp) and the Specific Thrust (TSFC)

1.1.1. Specific Impulse-

Specific Impulse or in short I_{sp}, is the characteristic which dictates the energetic efficiency of a propulsion system, as we can see in (Eq. 1), it dictates how much thrust we gain per mass unit of propellant per unit time. Consequently, one can see that for higher values of I_{sp} our propulsion system is more efficient in the sense of propellant utilization. Generally, airbreathing propulsion systems present way better I_{sp} performances, this because the propellant in an airbreathing systems is only the fuel, which has relatively low mass flow rates, opposed to a rocket which carries its oxidizer with it throughout the flight, so the propellant mass flow rate in it is relatively high. In Figure 1 we can see characteristic I_{sp} values for different propulsion systems and how they change with Mach number. On the same note we can state that the design of an airbreathing propulsion system is generally more complex, opposed to a rocket, because a rocket will give the same I_{sp} value for any velocity, opposed to an airbreathing system in which the I_{sp} changes drastically with the Mach number. Yet again, if designed properly, for a moderate range of Mach numbers, the airbreathing is way more efficient than conventional rockets.

For airbreathing engines, among them is the SFRJ, the I_{sp} is directly correlated to the air intake of the engine, that is because the relation between the thrust and the fuel mass flux, is one that allows lower fuel mass fluxes for the same amount of thrust as we increase the air

mass intake. For that reason, when dealt with very large air intakes, one can achieve I_{sp} that exceeds even 3000 seconds (prominent in turbojet engines). The SFRJ I_{sp} values are humbler than the ones in a commercial jet engine, but can reach values of around 1500 seconds in optimal conditions.

$$I_{sp} = \frac{F}{\dot{m}_p \cdot g_0} \tag{1}$$

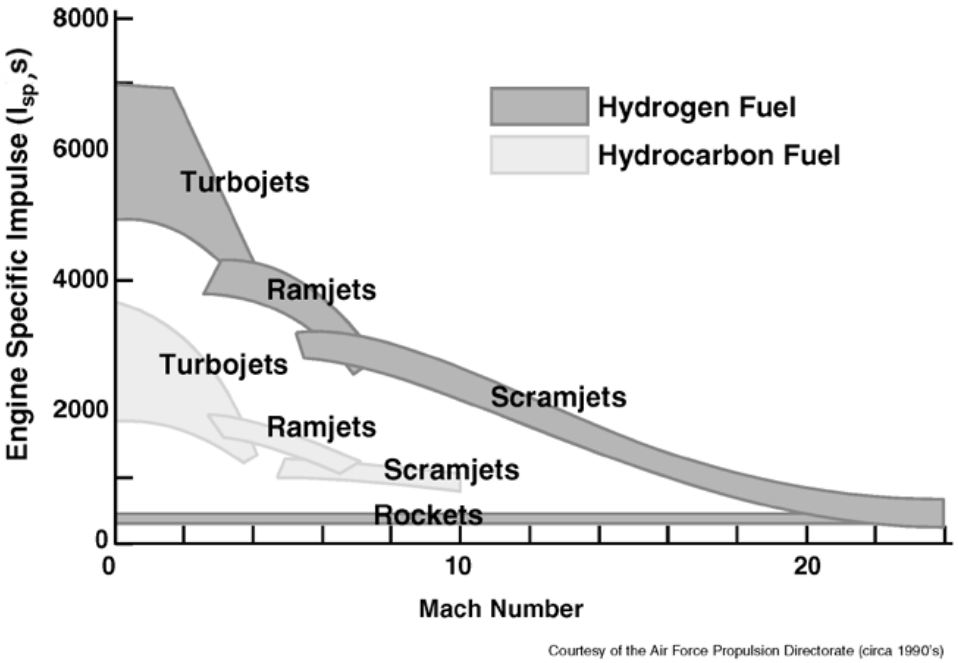

Figure 1- Characteristic I_{sp} values for different propulsion systems as a function of Mach number. Air Force Propulsion Directorate (circa 1990's)

1.1.2.Specific Thrust-

The specific thrust, is a characteristic which represents the thrust generated from a given inlet (thrust per airflow rate), correlated to the total ambient mass intake of the propulsion system ($F/\dot{m}_a$), this parameter indicates the maximum drag that a propulsion system can overcome, and consequently determines its maximal flight Mach. One can see that for rockets this parameter is essentially infinity because there is no air intake, and for airbreathing propulsion systems such as turbojets, or ramjets, it becomes low because of the large air intake. This characteristic helps us understand what minimal level of thrust is required for a specific flight mission, under dictated altitude and velocity profiles.

2. The Ramjet Engine

The ramjet engine is a type of an airbreathing propulsion system, which means that it carries its fuel but not its oxidizer. What differentiates the ramjet from other airbreathing propulsion systems is the fact that the ramjet does not have any moving parts like a compressor or a turbine, but it in fact uses the principle of aerodynamic compression for supersonic flight (oblique and normal shockwaves, depending on configuration) and expands the flow through a nozzle. Because of the compression efficiency of shockwaves, there are some limitations on the flight speed, and it was found that the ramjet engine becomes preferable in terms of energy efficiency from flight Mach number of about 2.5. After the air is compressed, it flows to the inlet of the combustion chamber. In the case of a solid fuel ramjet, the incoming air flows into the combustion chamber through a rearward step. The sudden expansion of the air forms a recirculation zone within the combustion chamber, which serves as a flame holder. The larger diameter of the combustion chamber, slows down the airflow, increasing its residence time inside the fuel grain, which increases the combustion efficiency and improves the flameholding properties. The flow within the combustion chamber is subsonic, typically up to Mach 0.5, hence, the static pressure of the flow is close to the stagnation pressure. After it reacts with the fuel within the combustion chamber, the reaction products flow through a converging diverging nozzle and expanded to about the ambient pressure, giving a supersonic exit jet that generates thrust. In Figure 2 we can see a diagram of a general ramjet operation.

From what we've discussed so far, we can see that the ramjet has large specific impulse, yet a relatively low specific thrust, which characterizes it with the ability to perform in longer ranges but not under a large drag (upper operation speed limit).

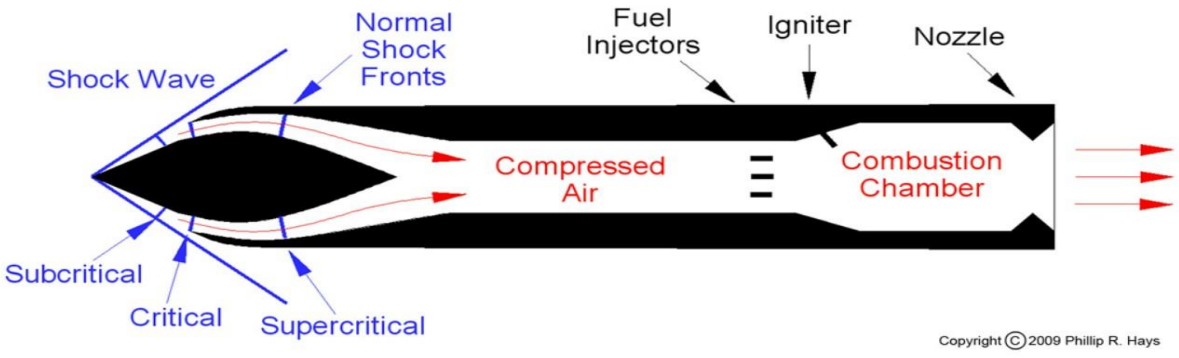

Figure 2- An operational scheme of a Ramjet engine. We can see the initial compression due to oblique shockwaves, and the secondary compression inside the inlet. Taken from Phillip R. Hays, circa (2009)

2.1. History and Applications

The ramjet concept first appeared in 1913 by René Lorin in France. Shortly after, in 1915, Albert Fonó proposed the idea of increasing artillery shells range utilizing ramjet technologies. 21 years later, in 1936, Trommsdorff submitted an idea for ram-pressured gun-launched projectiles, and eventually by 1938, they were used in 8.8mm anti-air guns (Trommsdorff, W., 1956) and were fired at velocity of Mach 2.5 (about 830 m/s). Afterwards the US took interest in ramjet technology and began experimenting with it. In January 1952, the US has conducted an experiment on a solid fuel rocket launched ramjet, the velocity range was 1.8-2.1 Mach. Afterwards a lot of experimental work was done by the US (NACA-NASA) and the Soviet Union, but it was only in the 60's where the soviets applied these concepts into operational weapons and introduced the SA-4 (Figure 3) and its more advanced counterpart, the SA-6 (Figure 3), which were proven very effective in combat against maneuverable targets. Through the years more countries started participating in research and military applications of ramjet technologies, which gave birth to missiles such as the British Bloodhound (SAM), the European Meteor (AAM), and the Russian P-800 Oniks (AShM), commonly known as Yakhont. (Veraar et al., 2021)

Figure 3- In this figure we can see the Ramjet AA systems, SA-4 (on the left), and SA-6 (on the right).

But the applications of ramjet technologies can be used to the likes of solid-fuel high-caliber gun-launched projectiles. Feasibility of SFRJ technologies for 35mm rounds was proven by TNO-RWMS, and the same was shown for 155mm SFRJ projectiles by RDM. The South African company Denel has researched the expected range for another type of SFRJ 155mm ramjet projectiles, and it showed an immense improvement in range over the conventional artillery shells used today [2] (Figure 4). There are some difficulties utilizing such propulsion systems, starting with a relatively low fuel regression rate (effects thrust) and specific thrust, moreover, the extreme loads acting on the fuel grain in the gun muzzle (~10000g) can cause

deformations and cracks, and hurt the performance of the fuel. Hence our motivation is to investigate the performance and characteristics of such propulsion systems, mainly from the point of internal ballistics.

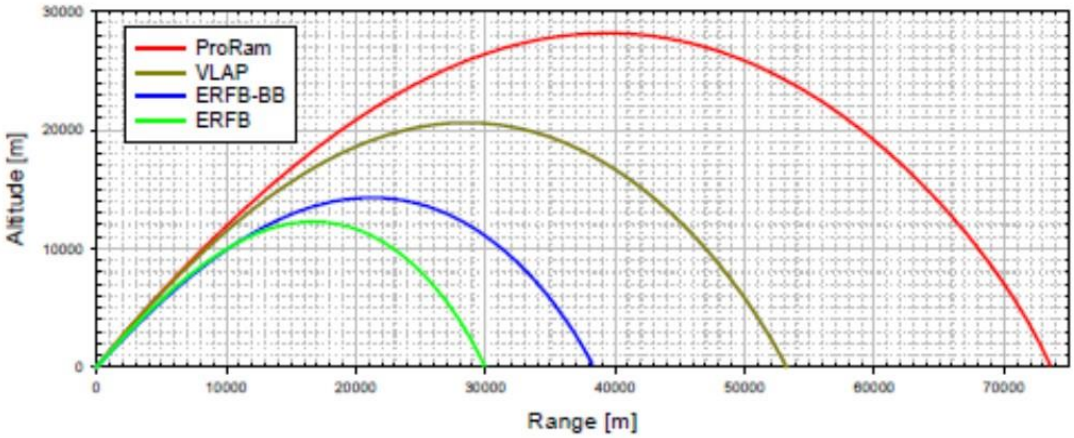

Figure 4- The expected trajectory of four different 155mm ramjet artillery shells. Taken from Verrar et al. (2021). ERFB (Extended Range Full Bore) is introduced in green and blue, with and without base bleed. VLAP (Velocity enhanced Long Range Artillery Projectile) is a form of guided artillery munition and introduced in brown. ProRam in red, is a projectile utilizing guided ramjet artillery. So, as we see, the expected range of ramjet artillery far exceeds these of other forms of artillery.

2.2. Solid Fuel Ramjet

The solid fuel ramjet (SFRJ) is the simplest airbreathing propulsion system there is, it does not contain any moving parts and consists only of a diffuser, a combustion chamber, and a nozzle. The SFRJ is kind of the opposite to a solid propellant rocket from the perspective of oxidizer utilization, while the solid propellant rocket carries all its oxidizer inside the tank, the SFRJ gets its oxidizer flow from the atmosphere resulting in much higher specific impulse (800-1000 s in SFRJ and 200-240 s in a rocket). For most cases the fuel is generally a hydrocarbon (HTPB, Polyester or else) and it is placed as a hollow cylinder in the combustion chamber, while for oxidizer we are utilizing the air flow through the fuel port. From handling perspective, we can see that in case of SFRJ, the fuel storage and thermal insulation of walls are a lot easier than in the case of a liquid fuel combustor. Due to the flame-holding characteristics of the engine, it is required to place a step at the inlet of the combustion chamber for sudden expansion and slowing of the incoming air. Another major problem that we face when operating a SFRJ is the lack of control over the Fuel-To-Air ratio (f) due to the lack of control over the fuel regression rate, which is affected by various properties of the air and flight such as Reynold number (Re), mass flow rate, mass flux, inlet air temperature and the port diameter which all change along the flight, in order to tackle this problem it was suggested to add expendable graphite (EG) to improve the fuel regression rate [3]. In the case of solid fuel combustion, and SFRJ is not an exception, we run into the phenomenon of gas-

phase diffusion flame over the surface of the solid fuel, which may result in poor combustion efficiencies. On the matter of gun launched SFRJ projectiles, it is also important to further discuss the type of fuel which we use, because for certain hydrocarbon fuels the specific thrust generated from engine would be insufficient to overcome the drag in the desired flight velocity, for such cases it is worth to consider the addition of certain metals such as Aluminum, Magnesium, and Boron to the fuel mix.

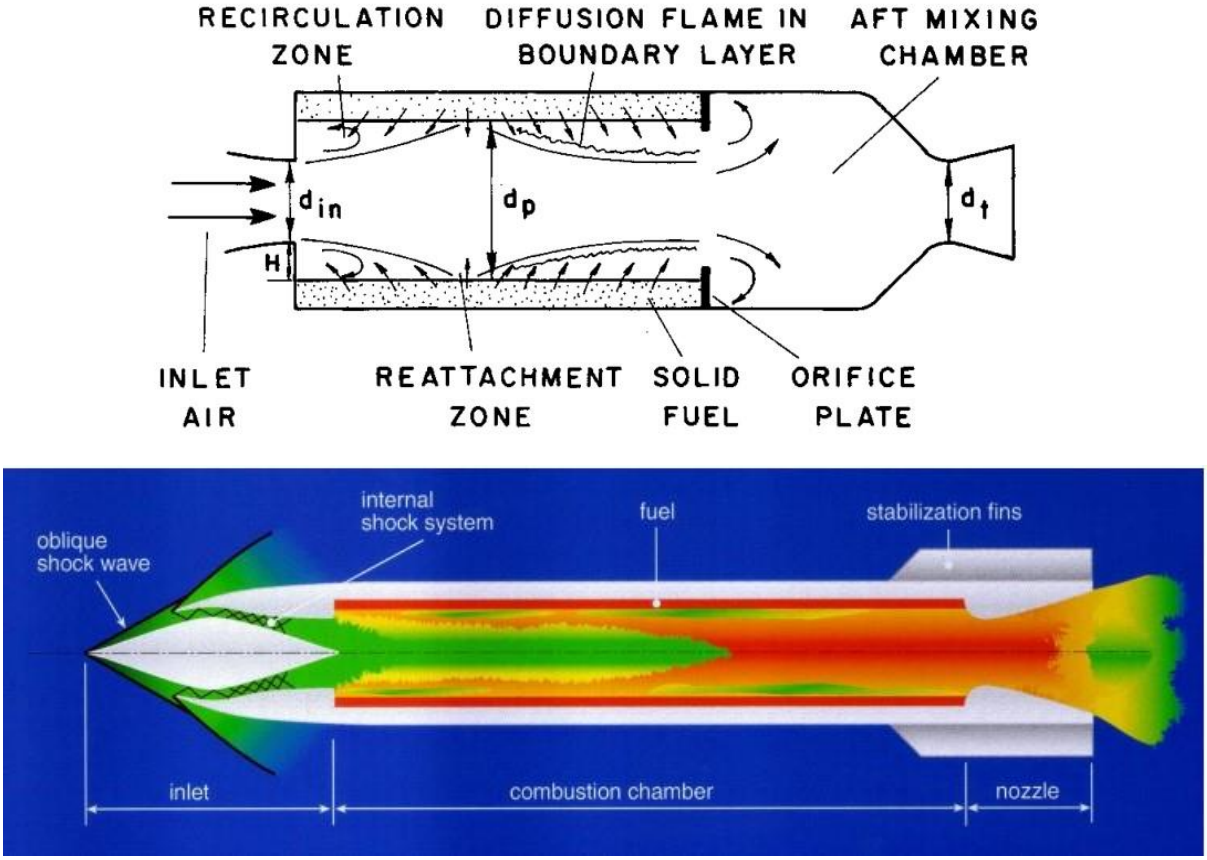

Figure 5- On the top we see a scheme of a Solid Fuel Ramjet Engine with an aft mixing chamber. Besides the mixing chamber, the other dimensions and regions are shared by all SFRJ's. Taken from (Netzer & Gany, 1991). On the bottom we see a CFD simulation of a SFRJ projectile combustion. We can see the recirculation zone right after the rearward step. Taken from (Veraar et al. 2021.)

The geometric features of a SFRJ consist of three main parameters, and the ratios between them, these are the inlet diameter (d_{in}), port diameter (d_p), and the throat diameter (d_t) as seen in Figure 5. We can take those parameters and reduce them to two dimensionless ratios that determine the flame-holding abilities of the SFRJ combustor, the ratios are $\frac{A_p}{A_{in}}, \frac{A_p}{A_t}$ when the first represents the inlet step height and the second represents the flow velocity inside the combustor. Using these two parameters we can characterize the entire combustor

configuration and determine its flameholding abilities for certain air temperatures as seen in Figure 6.

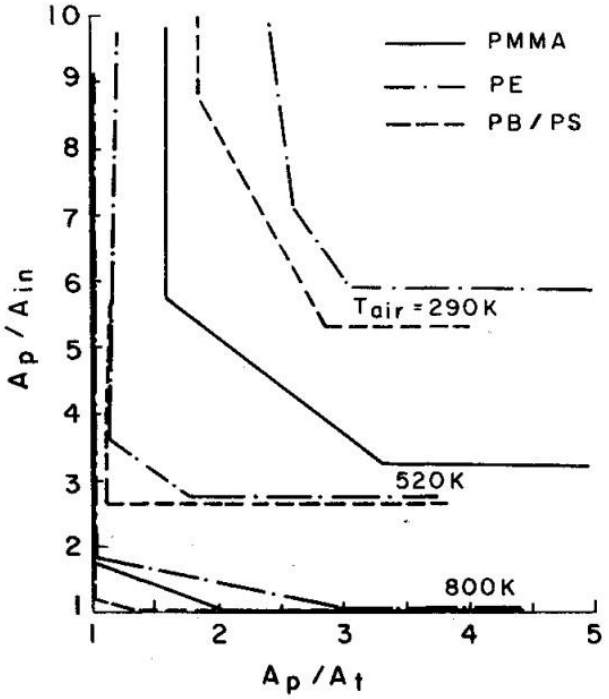

Figure 6- A map describing the flameholding capabilities of an SFRJ engine with correlation to the different geometric parameters of the engine, fuel type, and air inlet temperature (Netzer & Gany, 1991)

2.2.1.Gun Launched SFRJ Projectiles

Even though our discussion revolves around the feasibility of SFRJ projectiles. It's important to understand what our baseline is, which means, what are the gun launched projectiles that are used today, and what technologies are there to improve their performance.

The conventional projectiles used today (artillery shells, tank shells, rifle rounds) can be improved using some modifications, mainly to decrease the base drag coefficient (C_{D_b}). Such means are commonly referred as base-bleed (Fig. 7) and can achieve a reduction of 50% from C_{D_b}, and even more in the supersonic flight range (M>1.5) (Gany, 1991).

Active propulsion can be achieved for gun-launched projectiles using two methods. The first is a rocket motor (Rocket Assisted Projectiles or RAP in short), and the second one is an SFRJ motor. The rocket motor is very reliable, and many studies throughout history have helped us to thoroughly understand how it operates and what its limitations are. It is independent of flight conditions, but it has very high fuel consumption rates, which results in a poor specific

impulse, which limits the total momentum it can provide for the projectile. Additionally, it must be noted that the RAP contributes to large trajectory errors because of the propulsion independence relative to wind (Krishnan et al., 2000)

The second means to achieve active propulsion is SFRJ. The performance and characteristics of gun launched SFRJ projectiles were studied in the 90's, and even then, the superiority of the SFRJ in terms of energy, velocity, and accuracy, over RAP and base-bleed projectiles were prominent. The SFRJ seems to be a natural choice when discussing gun launched projectiles, the muzzle conditions will surely achieve the needed velocity for effective ramjet operation. The main advantage of SFRJ projectiles are their great velocities and high operation range (derived from the muzzle conditions and specific impulse). From the perspective of thrust-equal-drag flight, the projectile will maintain a ballistic trajectory of "vacuum conditions", helping to achieve high strike accuracy. Under such conditions it was seen that the SFRJ has trajectory self-correcting abilities against wind [6]. Due to the similar effect air density has, on both thrust and drag, the SFRJ can compensate for atmospheric variations in flight and maintain thrust-equal-drag state. It was also found that when considering the ballistic trajectory of an SFRJ round against a conventional one, the ramjet trajectory is "flatter", and closer to a linear trajectory, which will increase the aiming ability at small ranges of operation.(Gany, 1991.). (Fig. 9)

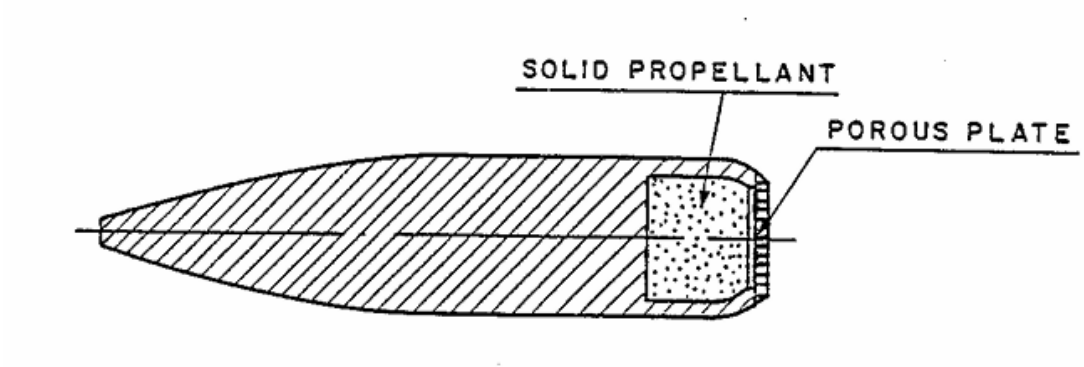

Figure 7- Scheme of a projectile with a base bleed system (Gany, 1991)

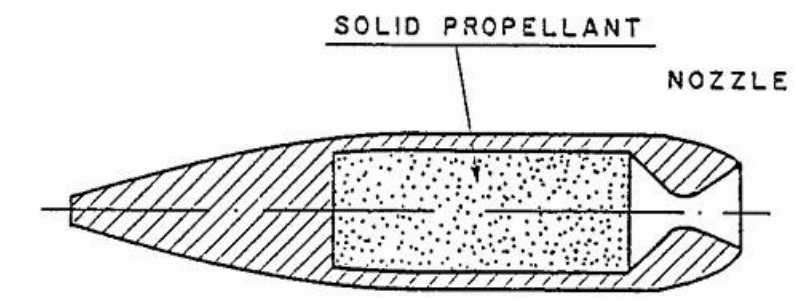

Figure 8- Scheme of a rocket assisted projectile (RAP) (Gany, 1991)

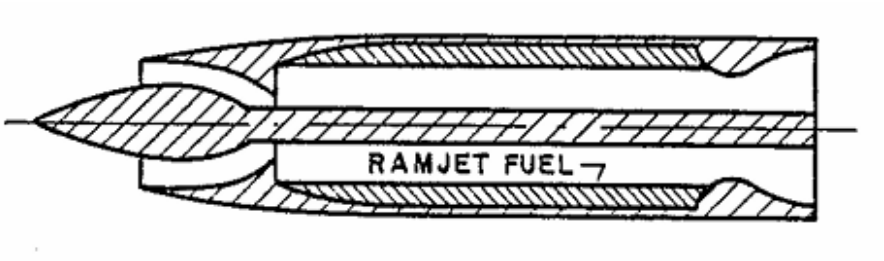

Figure 9- Scheme of an SFRJ projectile with a center-body configuration (Gany, 1991)

It is common to divide the gun launched projectiles into two main groups, which are derived from their operational use, and they are the Direct/Indirect Fire Systems (DFS/IDFS in short), when DFS is mostly used for smaller calibers, from 5.56 caliber rifles and up to 20-30 caliber anti-aircraft guns, when IDFS is mostly referring to different types of artillery such as mortars or cannons. A thorough study has been done by [8] on the subject of small scale SFRJ combustor which fits the description of a DFS projectile. This research, and further analysis had shown the feasibility of small caliber ramjet projectiles due to increase in energy, and trajectory performances (Gany, 1991). But today, the scope has shifted into the direction of IDFS's, and how to improve their performance (mainly from range perspectives but also accuracy). As we've discussed, the SFRJ seems like a good solution to this problem, due to high energetic efficiency, ability to balance out drag, and self-correcting properties against side winds.

When adding up all the advantages stated above, it seems that the ramjet is naturally "tailored" to be utilized for gun launched projectiles, sufficing high operational velocity and range, wind corrections, and a relatively flat ballistic trajectory, creating a very energetic projectile, with a trajectory easy to predict.

2.2.2. Thermochemistry

Since the ramjet is an air-breathing propulsion system, the thermochemical model is more complex than a simple rocket. As we will see, there is a great significance to the air properties at the inlet, as they affect the combustion properties and mechanism throughout the SFRJ operation. The two main challenges, when constructing a SFRJ engine for a certain mission, are the low fuel regression rate ($\dot{r}$), resulting in a relatively low thrust, and the flameholding capabilities of the SFRJ. In this section we will discuss these two challenges, and how we can overcome them, along with the main thermochemical properties of the SFRJ.

2.2.2.1. Flameholding Limits

The subject of flameholding in a SFRJ has been studied by a few people and gave great input on how we should approach the design of an SFRJ (A. Netzer & Gany, 1991b; Schulte, 1986), and it has been found that the limitations are affected mostly by the air temperature and interior velocity (residence time), fuel type, and the geometrical configuration of the combustion chamber. Which means, that for a certain mission, with dictated fuel type and flight conditions (ambient temperature), we can suffice sustained combustion, through a proper consideration of the different geometrical features of the combustion chamber, which includes the port diameter (D_p), step height (h), inlet diameter (D_{in}), and throat diameter (D_t).

The mathematical model of the flameholding mechanism is quite complex, depending on the heat transfer mechanism, which is dependent on the flow velocity, pressure, and geometry. But we have learned from experience that the flow at the beginning of the combustion chamber must be slowed down, to make sufficient contact time with the fuel grain and create combustion. As we discussed earlier, the slowing of the flow is done by a rear step at the inlet of the combustor, which creates a recirculation zone in which the combustion occurs. Studies have found empirical fits between the recirculation zone length (L_r) and the rearward step height (h), it was also found that there is no dependency on Reynolds number. The fits that were found are (D. W. Netzer, 1977, 1978; Elands et al., 1990):

- $L_r/D_p = -0.64 + 9.24h/D_p$
- $L_r/D_p = -0.73 + 11.93h/D_p$
- $L_r/D_p = -1.53 + 11.77h/D_p$

As we see, there is an increase of the recirculation zone length, along with the step height. This connection does make sense, since an increase of the step height will cause a greater expansion and slowing of the flow field, which results in longer contact time between the hot flow and the fuel grain which eventually causes combustion.

Furthermore, there is a significance to the throat diameter at the exit because it dictates the flow velocity in the combustion chamber. And now, even without diving deep and analyzing the full combustion model of the system, we can describe the flameholding capabilities via different geometric parameters of the engine.

It is common to describe the flameholding capabilities of a SFRJ, through two geometric ratios, which are, the ratio between the fuel-port area and the air-inlet area, $A_p/$

A_{in} (representing the step height), and the ratio between the fuel-port area to the throat area A_p/A_t (representing the gas flow velocity inside the combustor). It is important to represent the flameholding limits through non-dimensional parameters, since through that we can apply similarity on all SFRJ systems. As we've seen in Figure 6, through a series of 'go-no go' experiments, it is possible to create a map which describes the flameholding limit of the SFRJ and they change with temperature and geometry.

Given the general scheme for the flameholding limits of the SFRJ shown in Fig. 6, for given air inlet stagnation temperatures, theoretically, we can create a geometry that will fit within the flameholding map and hopefully satisfies the required flameholding capabilities. Yet again, we need to carefully consider the SFRJ design according to several parameters, which are not necessarily considered when revolving the discussion around the geometry of the engine.

First and foremost, when discussing gun-launched SFRJ, the projectile will have an outer design that will fit inside the gun barrel, which means that an outer diameter is always given. In this case, if we increase the fuel quantity, the port diameter will decrease, and if we increase the step, the port diameter will increase (effectively resulting in less fuel). The only parameter which we have somewhat full control over, is the nozzle throat diameter. When discussing the SFRJ design, from an operational standpoint, our top priority (aside from flameholding), is the fuel quantity, because a larger fuel quantity will result in a higher range. Which means that on the flameholding map, our working point will be as close as possible to the flameholding limit with minimal A_p/A_{in}, which indicates maximum fuel quantity and maximal operation time.

2.2.2.2. Heat Transfer and Fuel Regression Rate

One of the most interesting and complex limitations we must deal with in SFRJ performance is the fuel regression rate. The fuel regression rate in a SFRJ correlates directly to the thrust, and it is relatively low. The fuel regression mechanism itself is very complex. In addition to the mass flux or Reynolds number, it is affected by the step height, the axial distance, and the reattachment distance. The regression rate is minimal near the step, and maximal in the reattachment distance, which shifts through the operation of the SFRJ. The heat transfer mechanism plays a crucial part in the combustion process, but a few assumptions can be made to create a simplified model of the heat transfer and fuel regression rate.

In a conventional SFRJ, since the fuel is a cylinder, we can evaluate the combustion rate through the regression rate of the fuel diameter $\dot{r}$, and it is commonly represented by Eq. 2

$$\dot{r} = AG_a^n \tag{2}$$

When in this case, $'A'$ is a coefficient dependent on the different problem parameters, $'n'$ is an exponent, and G_a is the air mass flux, which in a SFRJ is approximately the same as the total exhaust mass flux, so Eq. 2 can be written as follows (Eq. 3).

$$\dot{r} = AG^n \tag{3}$$

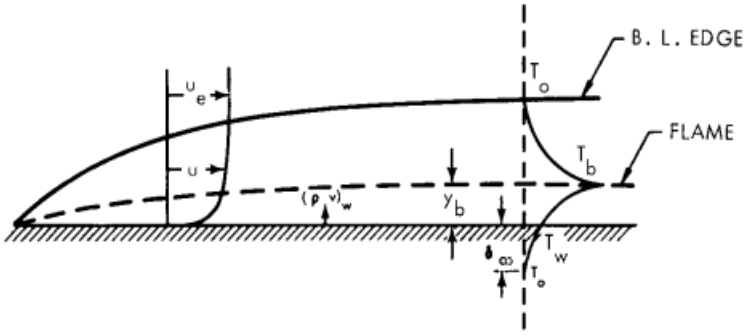

Figure 10- Scheme of a hybrid combustion, diffusion flame within the boundary layer (Marxman et al., n.d.)

The combustion process requires the gasification of the solid fuel, and only after that the combustion reaction can occur. Combustion occurs withing the gas boundary layer, at the area at which the oxidizer and gasified fuel flows are approximately at stoichiometric ratio [14](Fig 10). Several heat transfer processes dictate the gasification rate of the solid fuel wall, but a good assumption is to say that the dominant heat transfer mechanism, which is convection from the hot air flow, is the only heat transfer mechanism, which results in the next heat equation (Eq. 4) for the fuel regression rate.

$$\dot{r} = \frac{q_{conv}}{\rho_f h_v} \tag{4}$$

When q_{conv} is the convective heat transfer into the fuel wall, ρ_f is the fuel density, and h_v is the latent gasification heat of the solid fuel. The convective heat transfer can be expressed with the heat transfer coefficient h_c over a temperature difference as expressed in Eq. 5.

$$q_{conv} = h_c(T_c - T_w) \tag{5}$$

When T_c , T_w are the combustion and wall temperatures, respectively. Under the assumption of constant fuel to air ratio in the combustion, which results in constant combustion temperature, and moreover a constant wall temperature, the model can be further simplified, and the result are the relations shown in Eqs. 6,7.

$$q_{conv} \propto h_c \tag{6}$$

$$\dot{r} \propto h_c \tag{7}$$

As shown above, the conclusion is, that under certain combustion chamber operation conditions, the average fuel regression rate is heavily influenced by the heat transfer mechanism in the reattachment region (right after the rearward inlet step), or by the heat transfer mechanism downstream of the said zone. The heat transfer mechanism can be mathematically developed based on the model of a turbulent pipe flow. The boundary layer is turbulent and fully developed, and within it there is a constant temperature, constant phase, diffusion flame. One can apply the Reynolds analogy, between momentum and heat transfer, in a boundary layer and get. (Eq 8)

$$Nu \propto Re^n Pr^{0.33} \tag{8}$$

Where $Nu = \frac{h_c D_p}{k}$, $Re = \frac{\rho u D_p}{\mu} = \frac{G_a D_p}{\mu}$, $and\ P_r = \frac{C_p \mu}{k}$

So, equivalently, one can substitute the identities shown above into Eq. 9 and get,

$$\frac{h_c D_p}{k} \propto \left(\frac{\rho u D_p}{\mu}\right)^n \left(\frac{\mu C_p}{k}\right)^{0.33} \tag{9}$$

Isolating h_c will leave us with the next relation,

$$h_c \propto G_a^n D_p^{n-1} \mu^{0.33-n} C_p^{0.33} k^{0.67} \tag{10}$$

The flame in an SFRJ combustor takes place at a zone within the turbulent boundary layer, where the fuel/air ratio is approximately stoichiometric, hence the assumption of constant combustion temperature, and through operation this assumption is not bad; furthermore, the mass ratio between fuel and air through operation, assuming a solid hydrocarbon fuel, is typically between 2-6% of fuel mass to air mass. We need to remember that the flow moves through a combustion chamber, which means the chemical composition of the gas flow at the entrance and exit are different, pure air at the entrance, and air-fuel combustion products at the exit. But because of the mass ratio assumption, we can further simplify our thermochemical model and assume that all the flow within the combustion chamber is comprised only of air. Under this assumption we can determine the flow characteristics using Sutherland's law for k, μ (Eqs 11, 12).

$$\mu = 1.458 \cdot \frac{10^{-6} T_a^{1.5}}{T_a + 110.4} \left[\frac{kg}{m \cdot s^2}\right] \tag{11}$$

$$k = 1.993 \cdot \frac{10^{-3} T_a^{1.5}}{T_a + 112} \left[\frac{W}{cm \cdot K}\right] \tag{12}$$

We can add the assumption of linear variation of C_p with temperature (Eq. 13)

$$C_p = aT_a + b \tag{13}$$

For constant a , b

Substituting into Eq. 11 will result in the next equation for h_c (Eq. 14)

$$h_c \propto G_a^n D_p^{n-1} \left[\frac{T_a^{1.5}}{T_a + 110.4}\right]^{0.33-n} \cdot (aT_a + b)^{0.33} \cdot \left[\frac{T_a^{1.5}}{T_a + 112}\right]^{0.67} \tag{14}$$

The above equation can be represented in a simpler way, and after some algebraic manipulations we get (Eq. 15)

$$h_c \propto G_a^n D_p^{n-1} T_a^m \tag{15}$$

Using Eq.8, we can plug the relation shown above into the fuel regression rate, $\dot{r}$ (Eq. 16)

$$\dot{r} \propto G_a^n D_p^{n-1} T_a^m \tag{16}$$

This is an interesting result, because it implies that in a non-radiative system without blowing, the convective heat transfer mechanism, which in our case is the only heat transfer mechanism, and which is linearly correlated to the regression rate, under the assumption of constant air and wall temperatures, is affected only by the air mass flux, the port diameter, and the inlet air temperature. But as indicated beforehand, this relation is applicable only in case that the flow mechanism is a convective, turbulent pipe flow. But as we know, this is not always the case, when dealing with relatively low operation pressures in the combustion chamber, kinetic processes become prominent, and we should include the fuel regression sensitivity to the pressure. (Marxman et al., 1968.) has found that in a hybrid system of Oxygen and PMMA, that under a certain combustion pressure, the kinetic effects become prominent, but defining a certain threshold from which this phenomenon occurs proves difficult, but it seems that in the combustion pressure range of a conversional ramjet, the kinetic effects won't play a major part in the regression rate mechanism. Although the SFRJ and the hybrid systems are different, they only differ in their approach to oxidizer intake into the engine, while in Ramjet engines the oxidizer is ambient, in hybrid combustion we control the gaseous oxidizer flow. We do know that the combustion pressures in a SFRJ are inherently low, so we'll be tempted to think that the kinetic influence does exist, but we don't really know what is the limit from which this phenomenon happens. For the discussion, let us assume that such limit exists and that our working point is in a low enough combustion pressure. Under these circumstances, our equation will change and achieve the following form (Eq. 17).

$$\dot{r} \propto G_a^n D_p^{n-1} T_a^m p^b \tag{17}$$

As mentioned before, the heat transfer mechanism will be that of a pipe flow, with a fully developed, turbulent boundary layer. According to [15] under these assumptions we can assume that n=0.8, the temperature range is somewhere between 600-800K and m=0.14. Therefore, (Eq. 18).

$$\dot{r} \propto G_a^{0.8} D_p^{-0.2} T_a^{0.13} p^b \tag{18}$$

It's important to note that this analysis holds only in the case stated above, but in reality, we don't always find dependency on the above parameters or find a different correlation. In different studies the dominant parameters can vary a lot, for example, (A. Netzer & Gany, 1991) have found that the correlation with air temperature, is much more dominant, with an exponent of up to 0.9. For realistic experiments, it seems like the regression rate model is simpler, and mostly dependent on the oxidizer flux. Assuming the pressure is beyond the threshold in which kinetic effects are prominent, we can say that the other parameters, aside from the air flux,

does not have that great of an effect on the regression rate, but we cannot ignore them when considering the flameholding capabilities of the engine.

Up until now, the model described the heat transfer mechanism downstream of the reattachment region. Now we will turn to the heat transfer mechanism in the reattachment zone. In the reattachment region, the heat transfer reaches maximum, which means the Nusselt number (Nu) is maximal. [16] have experimented with the heat transfer rate within a pipe after a step (sudden expansion) and compared it to the one in a fully developed turbulent boundary layer far from the reattachment region. After them, [17] have experimented with the fuel regression rate showing that the variations in the heat transfer found by [16] correlate well with the fuel regression. Three interesting results were achieved from this study. At first, the value of the Nusselt number in the reattachment zone (Nu_{max}) can be directly correlated to the rearward step Reynolds number (Re_{in}), with characteristic length of $D_{in} = D_p - 2h$. The empiric connection is:

$$Nu_{max} \propto Re_{in}^{no} \tag{19}$$

Where 'no' is the mass flux exponent from the regression rate equation but in the reattachment region. An important conclusion from this relation, is that the heat transfer mechanism in the reattachment region is strictly dependent on the rearward step height (through Re_{in}), which is fundamentally different from the heat transfer mechanism in a fully developed boundary layer. Another important conclusion is that the relation between the heat transfer in the reattachment region ($Nu_{\max}$) and the one in a fully developed boundary layer downstream (Nu_{fd}), is increasing with the decrease of the port Reynolds number. And the correlation is as follows:

$$Nu_{max}/Nu_{fd} \propto Re^{-0.2} \tag{20}$$

From the definition of the port Reynolds number ($Re = \frac{D_p G_a}{\mu}$), one can conclude that the heat transfer effect of the reattachment region increases for a smaller port, which explains why it is easier to sustain combustion for higher D_p like we've seen in the flameholding section. In a case where there's a low grain passage Reynolds number, the dominant heat transfer mechanism will be the one in the reattachment region and it will dictate the heat transfer in the entire port. For low L_F/D_p ratios, when L_F is the fuel length, the aforementioned affect is further emphasized. The third conclusion is that there's an empiric connection between the heat transfer ratio, and the ratio h/D_p, and the heat transfer ratio increases with the increase in h/D_p. Under the assumption of constant Reynolds number, it can be shown that.

$$Nu_{max}/Nu_{fd} \propto \left(1 - 2h/D_p\right)^{-2/3} \tag{21}$$

Considering a situation in which Nu_{max}/Nu_{fd} is large, we can safely assume that the heat transfer mechanism is dominated by the reattachment region, and for the averaged problem variants over time, the next connection occurs:

$$Nu_{max} \propto Nu_{avg} \tag{22}$$

Another way to describe the rearward step Reynolds number.

$$Re_{in} = ReD_p/D_{in} = G_a D_p^2/(\mu D_{in}) \tag{23}$$

Substituting into eq. 19, 22 ,23, we can achieve another relation for the averaged Nusselt number in a system with a heat transfer mechanism dominated by the reattachment region.

$$Nu_{avg} \propto G_a^{no} D_p^{2no}/(\mu D_{in})^{no} \tag{24}$$

We can correlate this into a relation in terms of $\dot{r}$ (Eq. 25)

$$\dot{r} \propto G_a^{no} D_p^{2no-1} k/(\mu D_{in})^{no} \tag{25}$$

But this is not a generalized equation, we need to take into consideration situations in which the pressure and temperature play a part too. Which leads us to Eq. 26.

$$\dot{r} \propto G_a^{no} D_p^{2no-1} D_{in}^{-no} T_a^{mo} p^{bo} \tag{26}$$

We can use the values extracted from experiments for ‘no’ and ‘mo’. When it’s important to remember, that typically ‘no’ is about 2/3. At this point the discussion revolves around two distinct cases. The first case, in which the heat transfer mechanism is controlled by the flow downstream of the reattachment region, which is dictated by equation (19), and the second one, when the heat transfer mechanism is controlled by the flow inside the reattachment region which dictated by equation (26).

Yet the fact remains that the heat transfer model we were working with is applied only in a case in which the heat transfer is only convective, and without blowing. But because of the

change in the system geometry due to fuel regression, there will be blowing, and the heat transfer mechanism will change. In that case, it is common to add a correction factor to the equations. The correction factor is a thermodynamic factor, which means it is related to the combustion itself, and its value depends on the fuel-oxidizer mixture. One of the values of the factor for different oxidizer-fuel mixture is extracted from fuel regression experiments. In cases when blowing isn't negligible, the fuel regression rate due to radiation increases but at the same time the convective heat transfer to the wall decreases. But as we've stated before, relative to a hybrid engine, the fuel to air ratio in a SFRJ is much lower, which leads us to think that the blowing will be relatively low, and even negligible.

We've already introduced the simplistic model to the fuel regression rate, as dictated in Eq.3. Where 'A' is dependent on the different mission conditions, such as temperature, fuel type, and pressure, while the exponent 'n' is dependent on the heat transfer mechanism as described above, and the value does not necessarily follow the conclusions from the theoretical analysis, which means that the 'n' value for a heat transfer mechanism dominated by the downstream flow, can be lower than 0.8, or for the case of a heat transfer mechanism controlled by the reattachment region, higher than 2/3. (Korting et al, 1987). One can dive even further into the way in which the fuel regression is calculated, in terms of time averaging schemes, in our case they don't hold that great of an importance, but it's worth to mention that different time averaging schemes will result in different fuel regression rates for the same experiment.

A different approach to the fuel regression rate is based on the fuel geometry and gas mass flux in and out of the combustor. Defining the fuel-air mass ratio as 'f', and the fuel mass flux $\dot{m}_f$ will help us construct a relatively simple and intuitive model for the fuel regression. For a cylindrical fuel grain, with density of ρ_f.

$$\dot{m}_f = f \cdot \dot{m}_a \tag{27}$$

$$\dot{m}_f = \rho_f \pi L_f D_p \dot{r} \tag{28}$$

Now we can extract $\dot{r}$ (Eq. 30)

$$\dot{r} = \frac{f\dot{m}_a}{\rho_f L_f D_p \pi} \tag{29}$$

And through a bit of algebraic manipulation, we get.

$$\dot{r} = \frac{f \cdot \rho_a u_a (\frac{A_a}{A_{max}})}{4\rho_f \left(\frac{D_p}{D_{max}}\right) \cdot (\frac{L_f}{D_{max}})} \tag{30}$$

When A_a is the air capture cross section, and A_{max} is the maximum projectile cross section. In that way we can use the non-dimensional geometric relations, used to dictate the different heat transfer and flameholding relations, to describe the regression rate, and achieve an overall solid grip on the flammability, and fuel regression mechanisms, using the same parameters. We must not forget, that controlling the fuel regression rate in a SFRJ, means controlling the thrust, because maximizing the fuel regression rate, means working closer to the stoichiometric Fuel-To-Air ratio, this due to the fact that SFRJ engines work at relatively low Fuel-To-Air ratios, due to high intakes of air relative to the low fuel regression rates. More energetic combustion leads to higher exhaust velocity, which increases the thrust following the thrust equation. (Eq. 31).

$$F = \dot{m}_a[(1+f)U_e - U_a] \tag{31}$$

This equation holds under the assumption of an adapted nozzle, which is not a bad assumption in most cases, because normally, even if not adapted, the air expands to about 90% of the ambient pressure. Combining the relatively low ambient pressure and exit nozzle cross-sections, we can assume that the negative thrust addition from the pressure difference is negligible.

When implementing what was stated above to our case, it seems that in a SFRJ, which characterizes in relatively low fuel regression rates, it's important to properly characterize the heat transfer mechanism, between the one controlled by the reattachment region flow (short fuel grain length and small port diameter, results in a low Reynolds number), and its counterpart downstream of the said region (long fuel grain, large port, high Reynolds). As we've seen before, for each of these mechanisms the fuel regression behaves differently. Almost all the time the flight conditions, and the combustion working point, are given beforehand, and we don't have much control over them. It means that to increase thrust, we can either alter the geometry (A_a, A_{max}, D_p, L_f), change the fuel type, or use fuel additives (Mg, Al, B), which will discussed later.

2.2.2.3. Pressure Losses and Combustion Efficiency

When discussing energy utilization within the SFRJ it is important to address the combustion efficiency and pressure losses. The pressure loss is prominent in the SFRJ mechanism, or for that matter in any Ram type engine, due to aerodynamic compression, which, depending on the geometric configuration and flow velocity, can decrease the stagnation pressure by 30-50%. (Gany, 1991) have found, that utilizing center body geometry in the projectile, can increase the stagnation pressure recovery in about 50% (from about 0.4 p_0 to 0.6 p_0). This process can be further optimized, considering different nose geometries, and how they affect pressure recovery, shockwave configuration, and drag values.

After dealing with pressure losses, we need to focus on the combustion efficiency, which is a more intricate mechanism that depends a lot on the engine geometry. It is common to define the combustion efficiency as

$$\eta_{b_1} = \frac{T_c - T_{oa}}{T_{c,th} - T_{oa}} \tag{32}$$

When $T_{c,th}$ is the adiabatic flame temperature, T_c is the experimental flame temperature, and T_{oa} is the external air stagnation temperature which is calculated by.

$$T_{oa} = T_a(1 + \frac{\gamma - 1}{2} M_a^2) \tag{33}$$

M_a is the air Mach number which is defined by

$$M_a = \frac{u_a}{c_a} = \frac{u_a}{\sqrt{\gamma R T_a}} \tag{34}$$

T_c is determined by the experimental value of the characteristic velocity ($c_{ex}^{\star}$), which is defined by

$$c_{ex}^{\star} = \frac{p_c A_t}{\dot{m}_a + \dot{m}_f} \tag{35}$$

The characteristic velocity is a measure to the energetic potential of a certain fuel or propellant. Through the real value (c_{ex}^{*}) against the theoretical value (c_{th}^{*}) of the characteristic velocity we get a measure for the propulsion efficiency. Regarding Eq. 35, the term in the denominator is the exhaust flow rate. Practically we can only measure the air flow rate directly, but there are a few ways to measure the fuel mass flow, the main one is by weighing the fuel before and after the combustion and averaging the mass flow over time. The

theoretical value of the characteristic velocity ($c_{th}^{\star}$) can be calculated using different CEA (chemical equilibrium analysis) programs. Now that we have both terms it is also appropriate to define a second combustion efficiency, as the ratio between the characteristic velocities.

$$\eta_{b_2} = \frac{c_{ex}^{\star}}{c_{th}^{\star}} = \frac{p_c A_t}{(\dot{m}_a + \dot{m}_f) c_{th}^{\star}} = \sqrt{\frac{T_c}{T_{c,th}}} \tag{36}$$

One can see that in both cases, when the flame temperature reaches its adiabatic value, the efficiency will either way be one, and graphically, when substituting the typical values for each number, the graphs ($\eta_{b_{1,2,}}\ against\ T_c$) will be rather similar to each other, yet it's important to stick with one criterion.

The combustion efficiency varies wildly and can be increased by planning a proper combustor geometry, which can enhance the fuel and oxidizer mixing. It seems that combustion efficiency depends on three parameters. The first is the presence of an aft mixing chamber downstream of the combustion chamber, effectively allowing longer residence time within the engine, and for full combustion of the fuel. The second parameter is the step to port ratio (h/D_p), which we've discussed earlier, and the third is the equivalence ratio of fuel and oxidizer in the combustor. (A. Netzer & Gany, 1991) have shown that for a SFRJ projectile with a port diameter of 10mm, operating with nonmetallized solid fuels (PMMA, PE, PB/PS), high combustion efficiencies can be achieved (an average of 90%) through the additions of an aft mixing chamber with a mixer plate, and without it we can consider a few ways to increase the combustion efficiency, such as an increase in the step height. Metal additives, such as Li, Mg, Al, or expandable graphite can be used to increase the specific thrust, which plays a crucial part, considering the inherently low specific thrust values of a SFRJ.

Now we have covered an additional criterion which we must consider when designing an SFRJ combustor. Sometimes the different constraints on flameholding, combustion efficiency, and fuel regression align with each other, but it doesn't always necessarily mean that it is the case, and through a process of theoretical investigation, combined with a series of trial-and-error experiments, we can create the ideal geometrical configuration fit for our specific mission.

2.2.3. Internal Ballistics- Theory and Calculations

When utilizing an SFRJ engine, it's important to take note of the combustion performance at the desired work point, because energetic combustion effectively enhances our flight performance (specific impulse and thrust). Now one must think, how can we maximize the thrust of a given engine, ramjet or not. The first step is to think, how can we achieve the most energetic combustion possible, or in other words achieve a near stoichiometric Fuel-To-Air ratio. As we've seen in Eq. 31, the regression rate is directly correlated to the geometric properties of the engine, air mass flux, and flight conditions (stagnation air temperature, which depends on Mach number and ambient air temperature). But in Eq. 27 we see the regression rate is also correlated to the air specific mass flux G_a, which means it depends on the port area (D_p), air capture area (A_a), and the flight speed (u_a). From these two equations, and through a series of static firing experiments for a given engine, one can achieve the average Fuel-To-Air ratio (f) for a given fuel configuration and flight speed. After we have this correlation, we can dictate the optimal working point for our engine, and if the working point is given to us, we can change the geometric properties of the fuel to try and optimize the combustion. Another way to increase the combustion energetic properties is by adding fuel additives. The addition of fuel additives can be done to fulfill two purposes. One is to increase the fuel energetic characteristics, and this is done by adding metallic additives such as Boron and Aluminum (Jung et al., 2018), and other is additives which increase the fuel regression rate, by enhancing the heat transfer mechanism from the surface to the inside of the fuel grain, and this is done by adding materials such as Expandable Graphite (or EG in short), (Muller & Gany, 2022). Another way to increase the fuel regression rate is by changing the shape of the fuel port. Changing the cross-section of the fuel port changes the surface area of the fuel, and higher surface areas will yield in higher fuel regression rates. It's a common practice in solid rocket engines to use a star-shaped fuel grain, or multiple ports and it can be done also in SFRJ's (Veraar et al., n.d.). It was also found that in a hybrid motor acting on Polyester and Oxygen, a helical port configuration was able to increase the fuel regression rate in up to 400% (Dinisman et al., 2024). It should be stated that utilizing such complex grain configurations can cause further pressure losses, and lower the structural integrity of the fuel grain, which is supposed to withstand very high barrel acceleration. So it seems, that in the case of gun launched SFRJ projectile, it can be better to utilize a relatively simple yet rigid, grain configuration, and deal with the low regression rate through other means.

To find a general indication on our working point with a given fuel, even before starting with our own experiments, we can begin by estimating the fuel regression rate, based on previous studies in the field, while staying as close as possible to our experiment conditions. These values can be plugged into different CEA programs along with the exit geometry, and by that calculate the combustion conditions, and flight performances.

Now that we have covered the parameters that affect the SFRJ performance, we can perform the necessary calculations to try and foresee the results of our experiments. The flight conditions are for a chamber pressure of $p_c = 12\ atm$ air stagnation temperature of $T_a = 720\ K$, and flight speed of $u_a = 930\ m/s$ at sea level. The calculations were performed by the NASA CEA code. Before we present the results, we'll introduce the basic concepts of propulsion and their modifications onto the SFRJ engine.

2.2.3.1. Combustion Performance

We can calculate the combustion temperature (T_c) or the characteristic velocity (c^*_{th}) for a given fuel and oxidizer ratios at certain conditions. These calculations are done using the NASA CEA code. The calculations presented here are for Polyester and HTPB, without fuel additives (Fig 11, 12). The Polyester and HTPB chemical formulas are (respectively) $C_{10}\,H_8\,O_4$ and $C_{667}\,H_{999}\,O_5$. It's important to note that the combustion efficiency criterion that we're using (noted as η_c) is η_{b_2} shown in Eq. 36. We can see that although both fuels have around the same energetic properties at their respective stoichiometric combustion ratios, the HTPB peaks at around twice the air flow the Polyester peaks in, this is due to the difference in chemical composition of both fuels.

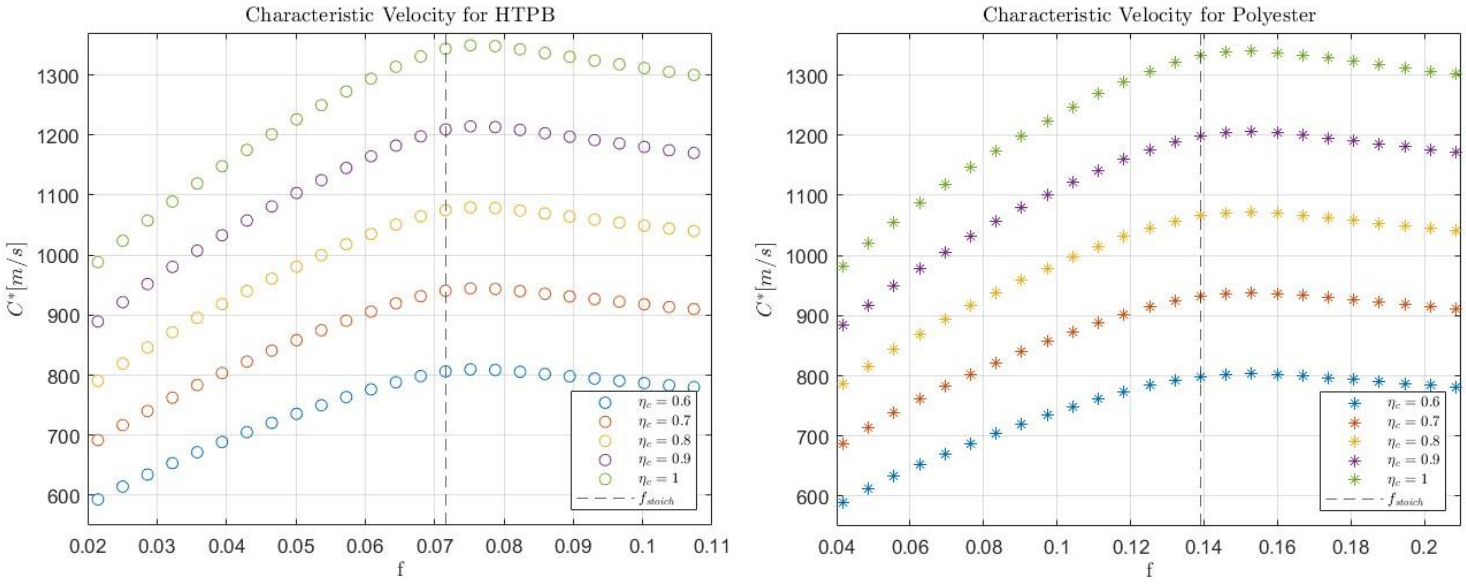

Figure 11- The theoretical Characteristic Velocity C^*_{th} vs the Fuel-To-Air ratio at different Combustion Efficiencies for two different solid fuel types (Polyester and HTPB)

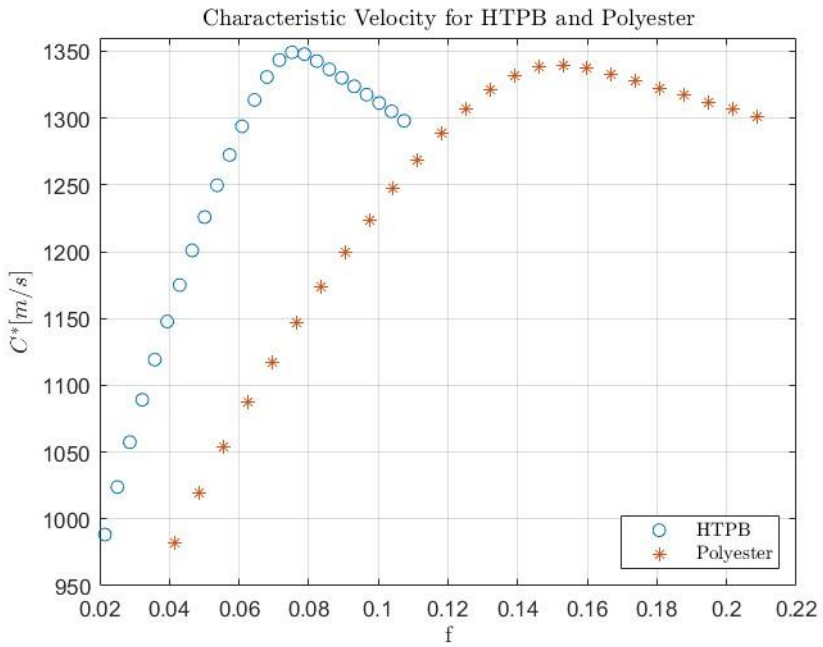

Figure 12- Here we can see C^*_{th} for Polyester and HTPB vs the Fuel-To-Air ratio f, with combustion efficiency (η_c) of 1. Due to different Chemical markup of the fuels, their C^*_{th} peaks at different fuel/air ratios.

2.2.3.2. Specific Impulse in SFRJ

The I_{sp} calculations were carried out using CEA. The CEA doesn't calculate the I_{sp} in seconds but it actually returns the exhaust velocity, considering the Combustion pressure and temperature, and the nozzle geometry. It's important to note that the CEA model is considered for a rocket, due to this, before we extract the I_{sp} from the program and deem it as the actual I_{sp}, we need to consider the entering momentum from the air intake. The flight velocity is known, and the exhaust velocity is calculated by CEA, utilizing equations (31,1), we can calculate the thrust and I_{sp}.

The I_{sp}, so as the thrust, are a function of both the combustion characteristics, and the exit nozzle. For that reason, it's important to take the exit nozzle geometry into account when calculating these characteristics. The calculations presented in this part are not for an adapted nozzle but for an area ratio that will better represent the real projectile, because allowing an adapted nozzle will mean an addition of extra friction drag and weight, so a common practice is to maintain an exit to throat ratio, A_e/A_t of about 2-3. In my calculations I've used an area ratio of 2.4. The calculations of the I_{sp} variation is presented below (Fig 13). The difference in I_{sp} for the different fuels is due to the difference in chemical composition of both fuels.

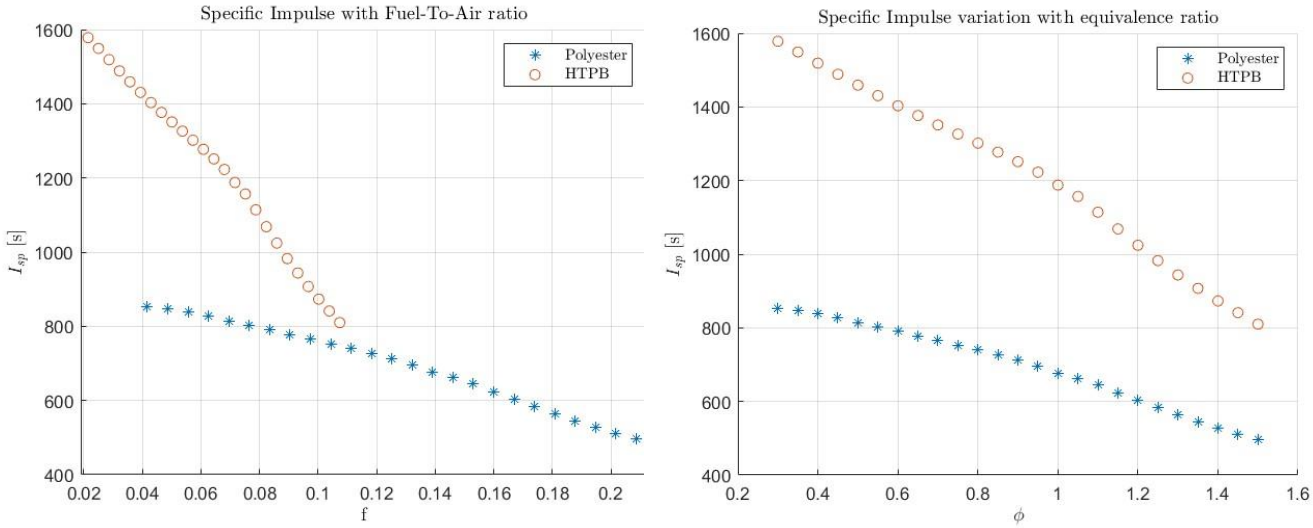

Figure 13- On the left, we can see I_{sp} for Polyester and HTPB with the change in the Fuel-To-Air ratio f. On the right we can see the I_{sp} change with the equivalence ratio ϕ.

2.2.4. External Ballistics

In this work we discuss the performance of gun-launched SFRJ projectile, therefore a discussion on the topic of external ballistics is necessary. We can divide gun-launched projectiles into many sub-categories, and our discussion will mainly revolve around Self-Propulsion.

2.2.4.1. Self-Propelled Projectiles - General description

Projectile launching performances strongly depend on the drag created through the flight, and how fast it can cancel out the initial momentum. In fast moving projectiles (rounds of all sorts), the aerodynamic drag, which is comprised mainly of skin-friction and wave drag, is one of the limiting factors of the projectile performance. Through the years, a few concepts have been developed to tackle this exact problem. A relatively simple concept fulfilling that purpose, which was mentioned briefly before in this work, is called 'base-bleed', it's mainly utilized in artillery, and it increases the projectile range by about 20-30%. Essentially what it does is expelling gas into the low-pressure area behind the projectile (Fig. 7) reducing the vortices and by this reducing the base drag (C_{d_b}) by about 30% (Gany, 1991). After the development of the base-bleed technology, it was realized that its efficiency is capped at the values stated earlier, and newer concepts came into the world, this is when the idea of 'self-propulsion' was born. Self-propulsion is a practice in which an engine is attached to the projectile, creates thrust, and by that cancels out the skin-friction drag and helps maintaining cruise flight around the original flight conditions. The cancel of the drag (or even some of it)

from self-propulsion systems, can help us achieve a dramatic increase in range. There are two main types of self-propulsion, the first is the 'Rocket Assisted Projectile' (RAP in short), and the second is a 'Ramjet Assisted Projectile'. Generally, self-propelled projectiles are assisted by solid motors because it's simply not economical to integrate a liquid Rocket or Ramjet onto an artillery shell or Anti-Aircraft munition. Self-propulsion has different objectives, depending on the projectile type, but in the end they all converge into the purpose of increasing the accuracy and energy performance of the projectile.

In this case, the natural way is to try and utilize the rocket engine, due to a fairly simple design, and reliable performance. Yet in-depth investigations have shown that utilization of RAP can be problematic. Besides high propellant consumption rates, which leads to low specific-impulse, it was found that when utilizing rocket propulsion onto different gun-launched projectiles, the deviation in trajectory increases with the projectile range. Another major, which is more prominent in short-medium operation ranges, for example anti-aircraft-ammunition or rifle rounds, it is simply not beneficial to add a rocket booster to each projectile, due to relatively low energy we can produce from the engine for such shorts flight times.

The type of engine that fits our requirements is the SFRJ, due to certain advantages it has over the solid rocket for our flight conditions. As an airbreathing engine it can balance out trajectory deviations caused by side winds and balance out the skin-friction drag with the thrust due to a linear proportion they both have with the air density. When a Thrust-Equal-Drag flight is achieved, we are in a state called 'pseudovacuum', in which the trajectory is very similar to a ballistic one, which makes it easier to aim and increase the accuracy of the projectile. Moreover, the thing that makes rocket assisted propulsion problematic for projectiles, is the fact that in long ranges, under the influence of winds, a small deviation in the flight angle relative to the wind, can cause a diverging moment in the projectile, and deviate it from its original trajectory. As mentioned before, since the ramjet engine is an airbreathing engine, it naturally overcomes said side winds, through the creation of balancing moment which aligns the projectile with the wind while maintaining its original flight trajectory. [5].

As we see in Fig 4, the potential of SFRJ gun-launched projectile is immense, and through a proper parametric investigation, and an optimization process of the internal ballistics, one can achieve a great improvement in the ballistic properties of the projectile, which means an increase in the range, and a trajectory closer to a ballistic one.

2.2.4.2. Railed and Smooth Bore and Their Effects

One of the limiting factors on the combustion and regression rates, is the difference between projectiles launched from a smooth bore (for example tank rounds), vs projectiles launched from a gun with a railed bore (high caliber artillery, rifle rounds). We should ask ourselves how the railing of the bore affects the projectile, how does it affect the stresses working on the exhaust nozzle, and most importantly, how does it affect the heat transfer and flame-holding mechanisms, that were discussed before. As we've seen before, due to the naturally low Fuel-To-Air ratios, it is crucial for us to try and improve the Fuel-To-Air ratio, hence the regression rate. There is no unambiguous conclusion on the effect that spin-stabilization has on the regression rate. (Von Wahlde, R. 1989) has found that a rifled gun bore decreases the fuel regression rate. The explanation to this phenomenon, is that due to the strong inertial forces, caused by the spin of the projectile due to rifling of the bore, the burnt air 'sticks' to the inner circumference of the fuel, which creates a lean boundary layer. On the other hand, [23] has found that the spin stabilization actually increases the regression rate by about 10%. Besides that, we do know, that using fuel additives such as Boron or Aluminum in spin-stabilized engines proves more effective due to longer residence time of the hot metals caused by the inertial forces. So even when considering the case presented by (Von Wahlde, R. 1989) we might be able to at least keep the fuel regression rate at its initial value through the use of metallic additives.

3. Experimental Setup and Testing Procedure

In the 'Methods' chapter, we'll be introduced to the experiment system, what it's comprised of and how's it utilized for our purposes. Moreover, we'll discuss the preparation of the fuel grains and solid propellants, the ignition mechanism, and the different measuring methods.

3.1. Main System Set Up

The experiment system is called 'direct-connected' ramjet. Due to high stagnation pressures and temperatures, there's a need to find a way and simulate these conditions for a static firing. For that purpose, we use a vitiated air heater. It burns hydrogen within the high-pressure airflow to increase the temperature and balances it out with oxygen to reach an intake gas mixture, which is chemically and kinetically similar to the theoretical ambient air at our working point. The major difference between our hot air, and natural hot air, is the fact that in our air there's 5% excess water vapor, caused by hydrogen combustion, leading to what is called 'wet air', and this is the air we're working with. The use of 'wet air' is a customary practice and is used in air heaters working at large mass flow rates.

After the air heater we reach a choked nozzle. The choked nozzle is used to create an aerodynamic separation between the engine and the air heater. When the nozzle is choked, we prevent the return of pressure waves back into the heater, which can cause damage to the different heater parts. After the choked nozzle we reach the engine, and at its exit there's a choked nozzle (Fig 14), which is the minimum requirement for a standard operation of a ramjet engine, because the air must expand to supersonic velocities. The diameter of the exit nozzle is planned by the required chamber pressure and mass flow rate, through the relation for a choked cylindrical port (Eq. 37)

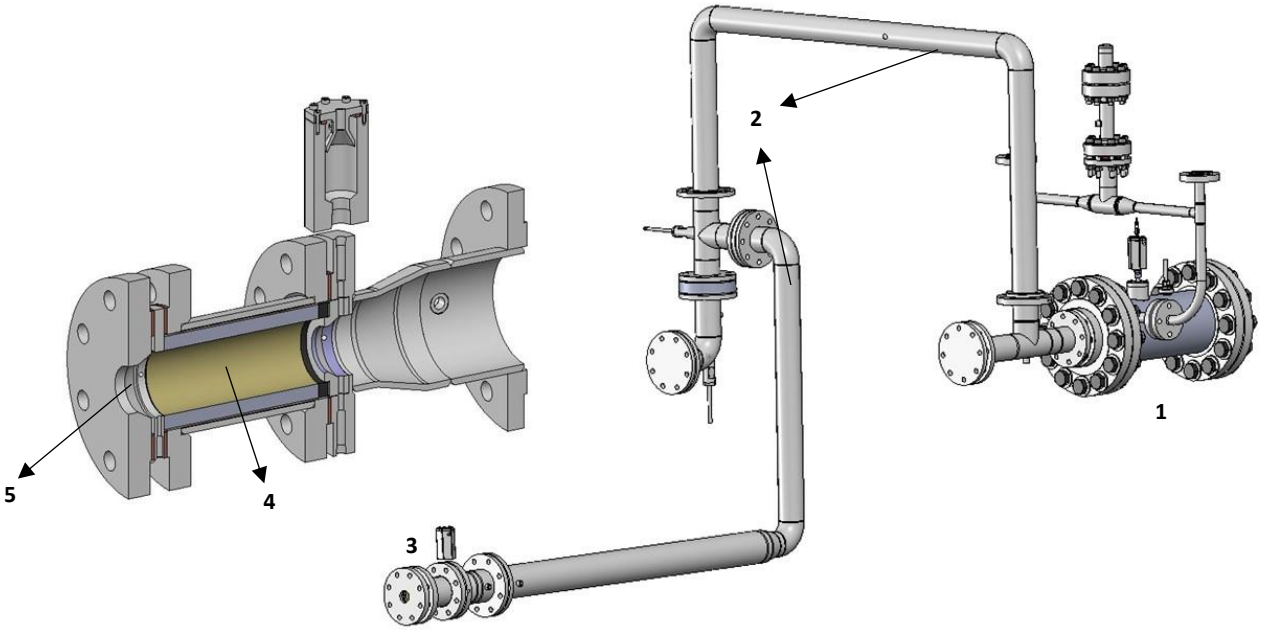

Figure 14- Here we see a scheme of the system setup. On the right we can see the air heater (1), and after it we see the system piping (2) which leads the pressurized air to the engine. And finally (bottom left) the engine itself (3). In the Left image we can see the engine's cross section, including the fuel grain casing (4), and the exit nozzle (5)

$$c^* = \frac{P_c \cdot A_t}{\dot{m}} \tag{36}$$

Where $c^*$is the characteristic velocity, which can be calculated via CEA considering the combustion efficiency and the fuel to air ratio. P_c is the combustion pressure, and A_t is the exit throat diameter.

3.2. Control and Data Gathering

The experiment data are gathered through a series of thermocouples and pressure gauges throughout the system (heater exit, choked nozzle, engine inlet, exit nozzle). The different gauges are connected to National Instruments analog cards and the data are analyzed using these cards and the LabView software, which also allows control over the different system

valves and the pressure of the inlet pressurized gasses (Oxygen, Hydrogen, Nitrogen, Air). (Fig 15).

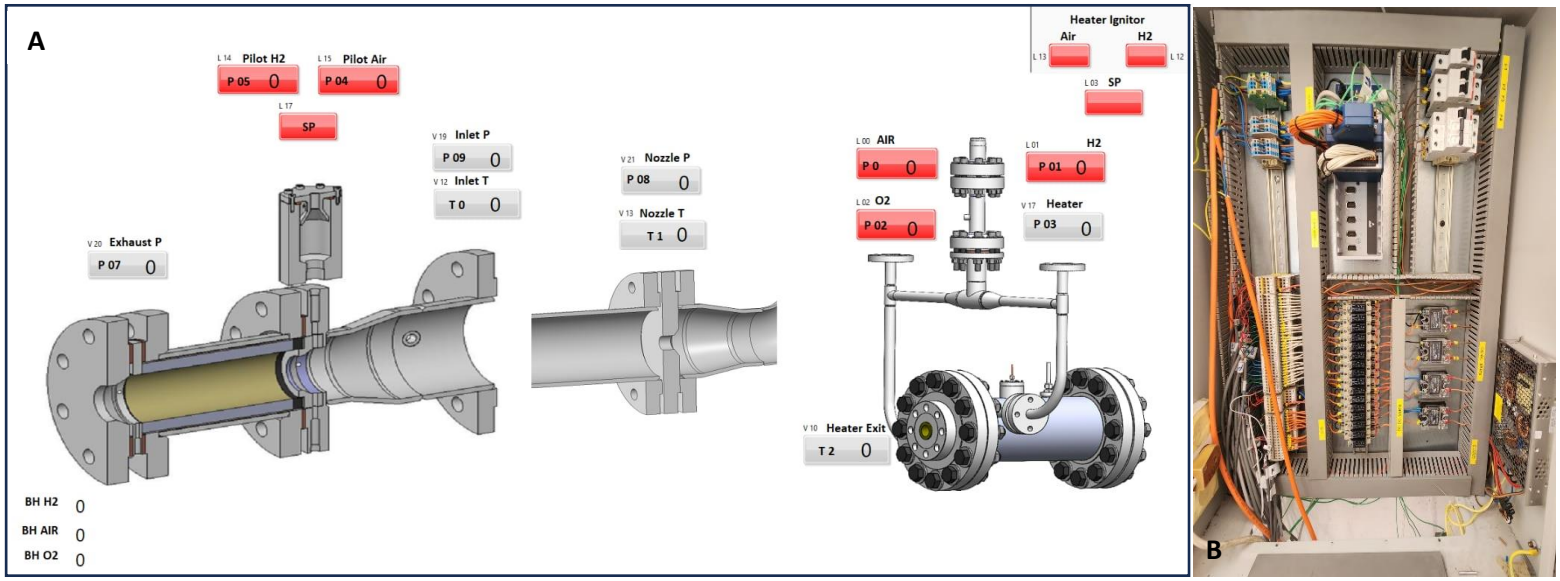

Figure 15- In Image 'A' we can see the experimental system LabView GUI screen. From the right to the left, we can see the air heater, the choked nozzle used for separation, and the engine itself, with inlet measurement, and exit nozzle measurement. In Image 'B' we can see the electric box and the cards used to connect the different gauges to the LabView control system.

3.3. Casting of the Fuel Grains

The fuel grains are hollow cylinders, and were supposed to fit inside a phenolic tube, used for insulation, and after that be put inside the engine. The casting of the fuel grains was a relatively simple method, comprised of 3D printing a mold out of ABS plastic, casting the liquid Polyester fuel (premixed with 1% hardener) inside the mold, waiting a few hours for it to harden, and finally melt the ABS plastic in Acetone. All in all, this process (printing, casting, melting) would take about a day per fuel grain. Because the molds are single-use, this process have proved to be not so efficient, due to the time it takes to print each mold, yet it is simpler than other methods that were practiced in the past, such as casting the fuel into metal mold and removing said mold once the Polyester starts to harden and becomes a gel-like state. This process, although sounds relatively simple, leads to an uneven surface of the fuel due to sticking of parts of the Polyester semi-hardened resin. A problem we had to tackle is the shrinkage of Polyester resin once hardened. The shrinkage is proportional to the surface area, Polyester amount, and hardener amount in a single mold. In our case, the shrinkage varied from 2-4.5% diameter decrease (inner and outer diameter of the fuel grain), which we had to consider when dictating the size of the mold, for the Polyester to eventually reach the

designated diameters. The dimensions of the fuel grain are an inner diameter of 60 mm and an outer diameter of 85.7 mm, with a combustor length of 169 mm. (Figures 16, 17)

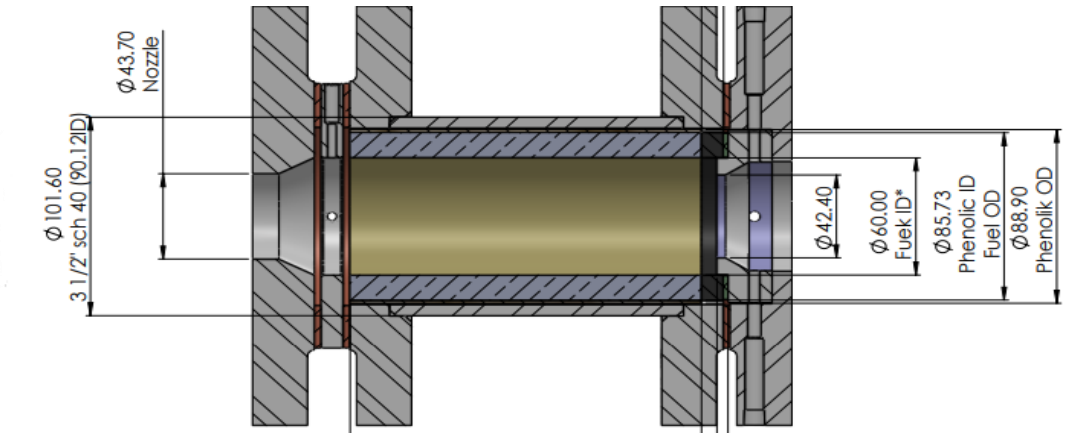

Figure 16 - The SFRJ engine Model, with a rearward inlet step of 9.3 mm, cylindrical fuel port dimensions, phenolic casing, and exit nozzle. The black ring at the inlet is solid propellant used for ignition, but it's configuration might change.

3.4. Ignition Method and the Casting of Solid Propellants

In our experiment, the method of ignition is not that important. When investigating the characteristics of an engine, one of the main criteria is its flameholding characteristics. If the flameholding characteristics of the engine are not good, it doesn't matter if ignition occurs, because the flame won't be able to sustain itself. For that matter, we've chosen to ignite the fuel using AP (NH_4ClO_4) based solid propellants. Due to the nature of Polyester fuels, and the fact that they undergo pyrolysis at around $900\ °C$, it seems that at our experiment working point (Air at $700 - 800\ K$), Polyester based propellants won't be reactive enough to ignite spontaneously from the hot air. For that purpose, we've chosen to use AP: HTPB based propellants, due to the relatively low pyrolysis point of HTPB ($300 - 400\ °C$). The casting of HTPB propellants is relatively simple yet a series of safety precautions need to be taken before casting (especially when casting the HTPB into solid propellants). The HTPB is mixed with a curing agent (IPDI), and a catalyst (DBTDL), afterwards we took the said mixture and mixed it with AP particles of $200\mu m$ at a ratio of 75:25 AP: HTPB. Industrial propellants are cast with AP particles of different sizes, but due to regulations we cannot use smaller size AP, which leads to ignition at higher temperatures for our propellants. The ignition temperature of our propellants should be around the cruise Mach stagnation temperature (around 700-730K), which is actually around the ignition temperature of said propellants (with only $200\mu m$ AP grains). The propellant was casted into rectangular shaped molds made out of ABS+ plastic

(similar to regular ABS, less rigid, not soluble in Acetone), and after curing the mold could be peeled off the propellant and glue the propellant onto the fuel grain. If ignition using solid propellant won't work, we can use a hot-gas pilot to ignite the flow using combustion of hydrogen and air. The problem with this ignition is that we have to intervene with the flow and by that we won't be able to simulate the combustion process as it would occur realistically. (Fig 17).

Figure 17- On the left image we see casted solid propellant, after being separated from its mold, the rough texture can be explained by insufficient mixing, showing some areas with high content of AP grains. On the right we see a casted fuel grain, after being separated from its mold and with solid propellant glued on.

Bibliography

[1] Trommsdorff, W., “High-velocity Free-Flying Ram-Jet Units (TR-Missiles) – Research Work at the German Army Ordnance”, *AGARD First Guided Missiles Seminar*, Munich, Germany, April 1956.

[2] Veraar, R. G., Oosthuisen, R., and Andersson, K.” Ramjet propulsion for projectiles, an overview of worldwide achievements and future opportunities”, *International Journal of Energetic Materials and Chemical Propulsion*, 2022

[3] Oosthuizen, R., Du Buisson, J. J., and Botha, G. F., “Solid fuel ramjet (SFRJ) propulsion for artillery projectile applications-concept development overview mechanical/structural design drive plug”, *19th International Symposium of Ballistics*, 2001, pp. 403-410.

[4] Muller, G. T., and Gany, A., “Expandable Graphite Effect on Solid Fuel and Propellant Combustion,” *FirePhysChem*, Vol. 2, No. 1, 2022, pp. 72–75. https://doi.org/10.1016/J.FPC.2021.12.001

[5] Gany, A., “Analysis of Gun-Launched, SFRJ Projectiles", IJEMCP 1(1-6) 1991, pp 289-309.

[6] Krishnan, S., George, P., and Sathyan, S., “Design and Control of Solid-Fuel Ramjet for Pseudovacuum Trajectories.” *Journal of Propulsion and Power*, Vol. 16, No. 5, 2000, pp. 815-822.

[7] Fink, M. R., “Aerodynamic Properties of an Advanced Indirect Fire System (AIFS) Projectile,” *Journal of Spacecraft and Rockets*, Vol. 19, No. 1, 1982, pp. 36–40. https://doi.org/10.2514/3.62201

[8] Gany, A., “Accomplishments and challenges in solid fuel ramjets and scramjets.” *International Journal of Energetic Materials and Chemical Propulsion,* Vol. 8, No. 5, 2008, pp. 421-446.

[9] Netzer, A., and Gany, A., “Burning and Flameholding Characteristics of a Miniature Solid Fuel Ramjet Combustor,” *Journal of Propulsion and Power*, Vol. 7, No. 3, 1991, pp. 357–363. https://doi.org/10.2514/3.23334

[10] Schulte, G., “Fuel Regression and Flame Stabilization Studies of Solid-Fuel Ramjets,” *Journal of Propulsion and Power*, Vol. 2, No. 4, 1986, pp. 301–304. https://doi.org/10.2514/3.22886

[11] Netzer, D. W., “Modeling Solid-Fuel Ramjet Combustion,” *Journal of Spacecraft and Rockets*, Vol. 14, No. 12, 1977, pp. 762–766. https://doi.org/10.2514/3.27994

[12] Netzer, D. W., “Model Applications to Solid-Fuel Ramjet Combustion,” *Journal of Spacecraft and Rockets*, Vol. 15, No. 5, 1978, pp. 263–264. https://doi.org/10.2514/3.57316

[13] Elands, P. J. M., Korting, P. A. O. G., Wijchers, T., and Dijkstra, F., “Comparison of Combustion Experiments and Theory in Polyethylene Solid Fuel Ramjets,” *Journal of Propulsion and Power*, Vol. 6, No. 6, 1990, pp. 732–739. https://doi.org/10.2514/3.23279

[14] Marxman, G. A., Wooldridge, C. E., and Muzzy, R. J., Fundamentals of hybrid boundary-layer combustion.” *Progress in Astronautics and Rocketry,* Vol. 15, 1964, pp. 485-522

[15] Krishnan, S., and George, P., “Solid fuel ramjet combustor design.” *Progress in Aerospace Science,* Vol. 34, 1998, pp. 219-256.

[16] Krall, K. M., and Sparrow, E. M., “Turbulent Heat Transfer in the Separated, Reattached, and Redevelopment Regions of a Circular Tube,” *Journal of Heat Transfer*, 1966, pp. 131-136.

[17] Zvuloni, R., Gany, A., and Levy, Y., “Geometric Effects on the Combustion in Solid Fuel Ramjets,” *Journal of Propulsion and Power*, Vol. 5, No. 1, 1989, pp. 32–37. https://doi.org/10.2514/3.23111

[19] Jung, W., Baek, S., Park, J., and Kwon, S., “Combustion Characteristics of Ramjet Fuel Grains with Boron and Aluminum Additives,” Vol. 34, 2018, pp. 1070–1079. https://doi.org/10.2514/1.B36919

[21] Dinisman, S., Eisen, N. E., and Gany, A., “Enhancing hybrid motor thrust by a helical-port fuel grain” *International Journal of Energetic Materials and Chemical Propulsion*, Vol. 23, No. 1, 2024, pp. 69-84

[22] Von Wahlde, R. “Design and Finite-Element Analysis of a Sabot for a 60mm Flared Ramjet” *US Army Ballistic Research Lab Aberdeen*, BRL-MR-3782, 1989.

[23] Tahsini, A. M., “Regression Rate Response in Spin-Stabilized Solid Fuel Ramjets,” *Journal of Mechanics*, Vol. 37, 2020, pp. 37–43. https://doi.org/10.1093/jom/ufaa012